Monatshefte für Chemie - Chemical Monthly
https://doi.org/10.1007/s00706-019-02493-5

ORIGINAL PAPER

Identification of protein kinase fibroblast growth factor receptor 1 (FGFR1) inhibitors among the derivatives of 5-(5,6-dimethoxybenzim idazol-1-yl)-3-hydroxythiophene-2-carboxylic acid

Galyna Volynets[1] · Sergiy Lukashov[1] · Iryna Borysenko[1] · Andrii Gryshchenko[1] · Sergiy Starosyla[1] · Volodymyr Bdzhola[1] · Tetiana Ruban[1] · Anna Iatsyshyna[1] · Lyubov Lukash[1] · Yaroslav Bilokin[2] · Sergiy Yarmoluk[1]

Received: 7 June 2019 / Accepted: 5 August 2019

Abstract
Fibroblast growth factor receptor 1 (FGFR1) plays an important role in tumorigenesis, suggesting that inhibitors of this protein kinase may become important compounds for the development of anticancer agents. Using molecular docking approach, we have identified a novel class of FGFR1 inhibitors belonging to the derivatives of 5-(5,6-dimethoxybenzimidazol-1-yl)-3-hydroxythiophene-2-carboxylic acid. It was revealed that the most promising compound 5-(5,6-dimethoxybenzimidazol-1-yl)-3-[2-(methanesulfonyl)benzyloxy]thiophene-2-carboxylic acid methyl ester inhibits FGFR1 with an IC_{50} value of 150 nM in in vitro kinase assay. The structure–activity relationships have been studied, and the binding mode of this chemical class has been proposed.

Graphic abstract

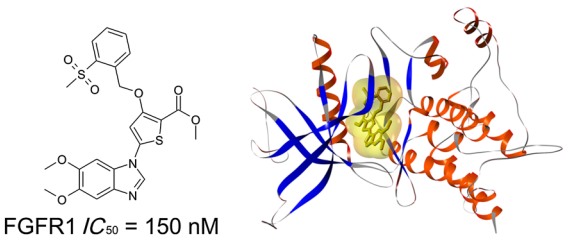

Keywords Drug research · Virtual screening · Kinase assay · Phosphorylations · Structure–activity relationships

Introduction

Fibroblast growth factor receptor 1 (FGFR1) is a transmembrane receptor tyrosine kinase which plays an important role in the regulation of cell survival, proliferation, differentiation, migration, and angiogenesis [1]. A number of experimental results clearly show that this protein kinase is involved in tumorigenesis. In particular, FGFR1 amplifications have been identified in lung cancer [2, 3], oral tongue squamous cell carcinoma [4], sinonasal cancer [5], gastric cancer [6], pancreatic ductal adenocarcinoma [7], colorectal cancer [8], etc. FGFR1 rearranged neoplasms lead to acute myeloid leukemia, T or B acute lymphoblastic leukemia, and mixed phenotypic acute leukemia [9, 10]. Therefore, FGFR1 is an important therapeutic target for the treatment of cancer diseases.

To date, the small-molecular inhibitors of protein kinase FGFR1 have been reported among the derivatives of 2-benzamido-4-(6-oxy-*N*-methyl-1-naphthamide)pyridine [11], 4-bromo-*N*-(3,5-dimethoxyphenyl)-benzamide [12], pyrrolo[2,3-*b*]pyrazine [13, 14],

Electronic supplementary material The online version of this article (https://doi.org/10.1007/s00706-019-02493-5) contains supplementary material, which is available to authorized users.

✉ Galyna Volynets
g.p.volynets@imbg.org.ua; galina.volinetc@gmail.com

[1] Institute of Molecular Biology and Genetics, the NAS of Ukraine, 150 Zabolotnogo St., Kiev 03143, Ukraine

[2] OTAVA Ltd., 400 Applewood Crescent, Unit 100, Vaughan, ON L4K 0C3, Canada

Published online: 28 September 2019

indazole [15–18], 3-(5′-substituted)-benzimidazolyl-5-[1-(3,5-dichloropyridin-4-yl)ethoxy]-1*H*-indazole [19], [5-amino-1-(2-methyl-3*H*-benzimidazol-5-yl)pyrazol-4-yl](1*H*-indol-2-yl)methanone [20], thienopyrimidine [21–24], pyridine-3-amine [25], 1*H*-pyrazolo[3,4-*b*]pyridine [26], 2-oxo-3,4-dihydropyrimido[4,5-*d*]pyrimidinyl [27], *N*-phenyl-*N*′-[4-(5*H*-pyrrolo[3,2-*d*]pyrimidin-4-yloxy)phenyl]urea [28], 5,7-dimethyloxazolo[5,4-*d*]-pyrimidine-4,6(5*H*,7*H*)-dione [29], 6-aryl-pyrido[2,3-*d*]-pyrimidine [30], 3-formylchromone [31], 3-vinylquinoxalin-2(1*H*)-one [32], pyrazolylaminoquinazoline [33], trichlorobenzene-substituted azaaryl [34], C-8 substituted guanine derivatives [35], oxindole and benzotiophene [36, 37], thiazol-2-amine [38], bisaryl-1,4-dien-3-one [39], naphthostyril [40], acenaphtho[1,2-*b*]pyrrole [41], 3-(3,5-dimethoxyphenyl)-1,6-naphthyridin [42], 4-[2,4-difluoro-5-(methoxycarbamoyl)phenylamino]pyrrolo[2,1-*f*]-[1,2,4] triazine [43], 5-amino-4-(1*H*-benzimidazol-2-yl)-phenyl-1,2-dihydropyrrol-3-ones [44].

Nowadays, several FGFR1 inhibitors are undergoing clinical studies [45, 46], but resistance to some inhibitors has already emerged. One of the mechanisms of acquired drug resistance in FGFR1 occurs through mutation of the hinge residue N546 and the gatekeeper residue V561 in the ATP-binding site of the kinase domain. N546K mutation can hinder drug binding by increasing affinity for ATP in comparison with the wild type. In addition, it was found that V561M mutation causes a significant reduction in affinity for highly potent FGFR1–3 inhibitor—PD173074 [47]. This finding provides the stimulus to search novel chemical classes of FGFR1 inhibitors.

Results and discussion

To discover the novel class of small molecule inhibitors for protein kinase FGFR1, we used a combination of computer modeling approaches and in vitro kinase assay. The virtual screening experiments were performed targeting the ATP-binding site of FGFR1 kinase by browsing commercially available OTAVA drug-like compound library containing about 100,000 ligands. According to docking results and visual inspection of the complexes of the best-scored ligands with amino acid residues of FGFR1 active site, 273 the most promising compounds were selected for biochemical screening. Among them, we have identified seven small-molecular inhibitors of FGFR1 carried 5-(5,6-dimethoxybenzimidazol-1-yl)-3-hydroxythiophene-2-carboxylic acid moiety close to IKKε inhibitor GSK319347A [48] and PLK1 [49] inhibitor.

Using molecular docking, it turned out that all compounds in this class display similar binding mode with the ATP-binding site of FGFR1 (Fig. 1). In accordance with the results of molecular modeling, benzimidazole is involved in the hydrophobic interactions with amino acid residues in the adenine-binding site. The nitrogen atom of this heterocycle forms a hydrogen bond with Ala564 located in the hinge region. In addition, carboxylic acid methyl ester forms a hydrogen bond with conservative Lys514, which is an important feature for the most of highly active FGFR1 inhibitors.

Several important structural features of 5-(5,6-dimethoxybenzimidazol-1-yl)-3-hydroxythiophene-2-carboxylic

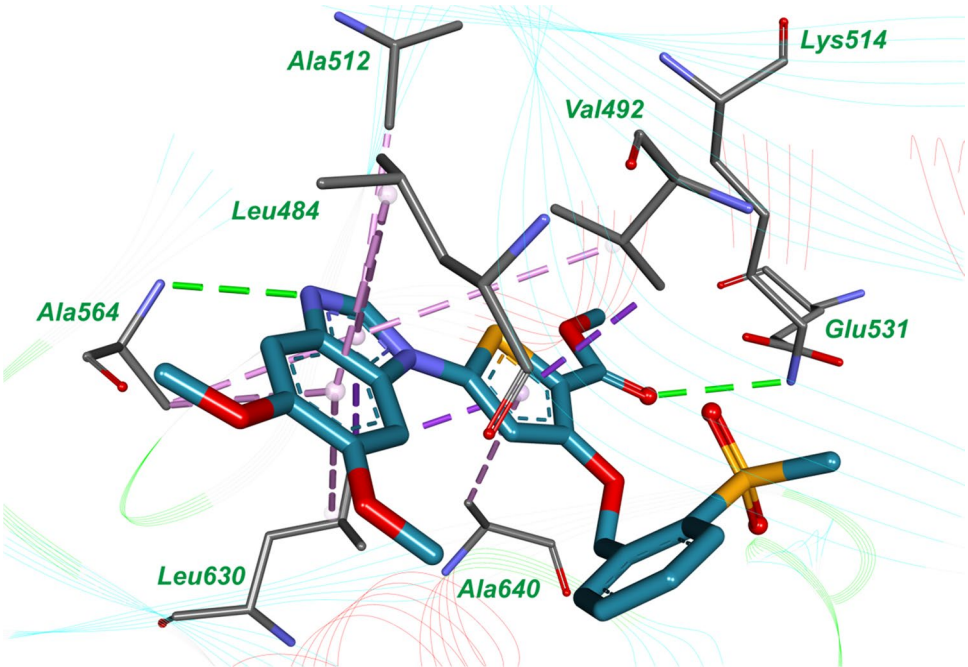

Fig. 1 Complex of compound methyl 5-(5,6-dimethoxy-1*H*-1,3-benzodiazol-1-yl)-3-[[2-(methanesulfonyl)-phenyl]methoxy]thiophene-2-carboxylate (**7b**) with amino acid residues in the active site of the FGFR1 catalytic subunit, obtained with molecular docking. Hydrogen bonds are shown by the green dotted lines and hydrophobic interactions are presented by the magenta dotted lines (color figure online)

acid derivatives were identified from a qualitative analysis of their activity on FGFR1 (Table 1).

The FGFR1 inhibitory activity of the studied derivatives depends on the structure of R^1 substituents in this heterocyclic system. We observed that compound **7b** with R^1 = methoxy group is more active (IC_{50} = 0.15 μM) than compound 5-(5,6-dimethoxy-1*H*-1,3-benzodiazol-1-yl)-3-[[2-(methanesulfonyl)phenyl]methoxy]thiophene-2-carboxamide (**8b**) with amino group (IC_{50} = 0.50 μM) or compound 5-(5,6-dimethoxy-1*H*-1,3-benzodiazol-1-yl)-3-[[2-(methanesulfonyl)phenyl]methoxy]thiophene-2-carboxylic acid (**8a**) with hydroxy group (IC_{50} = 0.50 μM) in this position, while the replacement of methoxy group (compound methyl 5-(5,6-dimethoxy-1*H*-1,3-benzodiazol-1-yl)-3-[[4-(methanesulfonyl)phenyl]methoxy]-thiophene-2-carboxylate (**7c**)) to dimethyl amine (compound 5-(5,6-dimethoxy-1*H*-1,3-benzodiazol-1-yl)-3-[[4-(methanesulfonyl)phenyl]methoxy]-*N*,*N*-dimethylthiophene-2-carboxamide (**8c**)) positively impacts the inhibitory activity (IC_{50} values are 5 and 3.7 μM, respectively). From the obtained results, the order of potency for the substituent R^1 could be proposed as follows: dimethyl amine > methoxy group > amino group > hydroxy group.

The nature of R^2 substituent also significantly affects the inhibitory activity towards FGFR1. We observed that compounds with R^2 = 2-(methanesulfonyl)benzyl are more active than those with 4-(methanesulfonyl)benzyl in this position. To compare this effect, one can refer to compound pairs such as **7b**, **7c**; **8a**, 5-(5,6-dimethoxy-1*H*-1,3-benzodiazol-1-yl)-3-[[4-(methanesulfonyl)phenyl]methoxy]-thiophene-2-carboxylic acid (**8d**) (corresponding IC_{50} values are 0.15 μM, 5 μM; 0.66 μM, > 30 μM). The compounds with hydrogen (methyl 5-(5,6-dimethoxy-1*H*-1,3-benzodiazol-1-yl)-3-hydroxythiophene-2-carboxylate (**6**)) and 3-hydroxythiophene-2-carboxylic acid methyl ester (methyl-5-(5,6-dimethoxy-1*H*-1,3-benzodiazol-1-yl)-3-[[4-hydroxy-5-(methoxycarbonyl)thiophen-2-yl]oxy]thiophene-2-carboxylate (**7a**)) have IC_{50} values equal to 0.56 and 23 μM, respectively. Therefore, based on the obtained results, the order of potency for the substituent R^2 could be proposed as follows: 2-(methanesulfonyl)benzyl > hydrogen > 4-(methanesulfonyl)benzyl > 3-hydroxythiophene-2-carboxylic acid methyl ester.

Therefore, substituents R^1 and R^2 in thiophene ring of 5-(5,6-dimethoxybenzimidazol-1-yl)-3-hydroxythiophene-2-carboxylic acid derivatives play a significant role for inhibitory activity towards FGFR1.

We have tested two the most active compounds **7b** and **8b** for antiproliferative activity against human T-cell lymphoblast-like cell line Jurkat. This cell line is characterized by high expression of FGFR1, FGFR4, and FGFR3 (FGFR1 expression is highest) [50]. The EC_{50} values are presented in Table 2. According to the results of in cellulo testing, the antiproliferative activity of compound **8b** was higher than in **7b** despite lower enzymatic potency, suggesting that compound **8b** has better membrane permeability. In addition, we have tested compounds **7b** and **8b** for cytotoxicity in

Table 1 Chemical structure of 5-(5,6-dimethoxybenzimidazol-1-yl)-3-hydroxythiophene-2-carboxylic acid derivatives and in vitro inhibitory activity towards protein kinase FGFR1

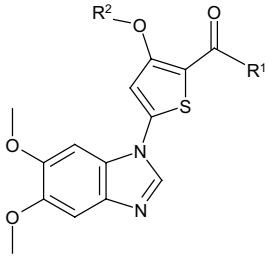

Compound	R^1	R^2	IC_{50} /μM
7b	OMe	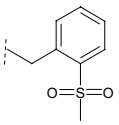	0.15
8b	NH_2	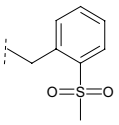	0.5
8a	OH	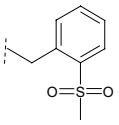	0.66
7c	OMe	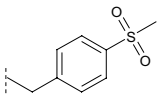	5
8c	$N(Me)_2$	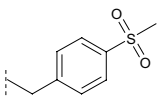	3.7
8d	OH	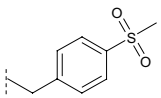	> 30
6	OMe	H	0.56
7a	OMe	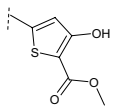	23

Table 2 Antiproliferative activities of compounds **7b** and **8b** against Jurkat and HEK293 cell lines

Compound	Jurkat cell proliferation EC_{50}/ μM[a]	HEK293 cell proliferation EC_{50}/ μM[a]
7b	215	> 250
8b	125	> 250

[a]Values are the mean of three independent experiments

"normal" non-tumorous cell line—HEK293. In this case, the compounds did not have effect on cell viability.

Conclusion

Therefore, the derivatives of 5,6-dimethoxy-1-thiophen-2-yl-1*H*-benzimidazole represent a novel class of FGFR1 inhibitors. The most active compound 5-(5,6-dimethoxy-benzimidazol-1-yl)-3-[2-(methanesulfonyl)benzyloxy]thiophene-2-carboxylic acid methyl ester (**7b**) inhibits FGFR1 with an IC_{50} value of 150 nM. According to the molecular docking results, the inhibitors from this class bind FGFR1 in such a way to form hydrogen bonds simultaneously with hinge region and conservative Lys514. The identified compounds can be used for further optimization of FGFR1 inhibitory activity and membrane permeability.

Experimental

Starting materials and solvents were purchased from commercial suppliers and were used without further purification. ^{1}H NMR and ^{13}C NMR spectra were recorded on a Varian VXR 400 instrument at 400 MHz. Chemical shifts are described as parts per million (δ) downfield from an internal standard of tetramethylsilane, and spin multiplicities are given as s (singlet), d (doublet), dd (double doublet), t (triplet), q (quartet), or m (multiplet). HPLC–MS analysis was performed using the Agilent 1100 LC/MSD SL separations module and Mass Quad G1956B mass detector with electrospray ionization (positive or negative ion mode as indicated) and with HPLC performed using Zorbax SB-C18, Rapid Resolution HT Cartridge 4.6 30 mm 1.8-Micron (Agilent P/N:823975-902) i.d. column, at a temperature of 40 °C with gradient elution of 0–100% CH_3CN (with 1 cm^3/dm^3 HCO_2H): H_2O (with 1 cm^3/dm^3 HCO_2H) at a flow rate of 3 cm^3/min and a run time of 2.8 min. Compounds were detected at 215 nm using a Diode Array G1315B detector. All purified synthetic intermediates and tested compounds gave 95% purity as determined by this method.

General synthetic procedure for 5-(5,6-dimethoxy-benzimidazol-1-yl)-3-hydroxythiophene-2-carboxylic acid derivatives

The addition of methyl thioglycolate (**1**) to methyl propiolate (**2**) in the presence of sodium methylate was followed with simultaneous cyclization into thiophene ring [51]. Mild chlorination of **3** with sulfuryl chloride gave chlorinated compound **4** [52]. Slow addition of **4** to benzimidazole **5** in homogeneous DMF solution induced an exothermic reaction that gave a complex mixture of products [49]. Therefore, **6** was isolated after chromatographic separation only with the yield of less than 30%. Among by-products was isolated compound **7a** bearing two thiophene moieties. Alkylation of **6** with corresponding benzylhalogenides in DMF using K_2CO_3 as a base gave almost quantitative yields of **7b** and **7c** that were converted into acids, and amides **8a**–**8d** under conditions, as indicated in Scheme 1. All synthesized compounds have ≥ 95% purity.

Methyl 5-(5,6-dimethoxy-1*H*-1,3-benzodiazol-1-yl)-3-hydroxythiophene-2-carboxylate (6, $C_{15}H_{14}N_2O_5S$) 18 g of 5,6-dimethoxybenzimidazole (**5**, 0.10 mol) and 17 cm^3 of triethylamine (0.12 mol) were dissolved in 150 cm^3 of dimethylformamide. Under stirring and cooling with cold water bath, 19.5 g of **4** (0.10 mol) were added portionwise. Stirring continued overnight, and then, 300 cm^3 of water were added and crude **6** was extracted with 3 × 100 cm^3 of methylene chloride. Combined organic layers were evaporated with 50 g of silica gel. Solid residue transferred into the top of 70 cm-long chromatographic column over 50 cm of SiO_2 and eluted with CH_2Cl_2/MeOH 95:5. After fractions contained rests of **3** and traces of **7a** fractions with product **6** were collected and evaporated to dryness giving 9.15 g (27%) of white powder. M.p.: 157–158 °C; ^{1}H NMR (400 MHz, DMSO-d_6): δ = 10.40 (s, 1H), 8.28 (s, 1H), 7.24 (s, 1H), 7.21 (s, 1H), 7.08 (s, 1H), 3.88 (s, 3H), 3.85 (s, 3H), 3.84 (s, 3H) ppm; ^{13}C NMR (75 MHz, DMSO-d_6): δ = 162.30, 159.76, 147.84, 147.06, 141.28, 140.74, 136.93, 134.02, 125.92, 112.52, 102.55, 93.97, 56.00, 55.92, 51.62 ppm; LC–MS (ESI): t_r = 0.845, m/z = 335.0 ([M + H]$^+$).

Methyl 5-(5,6-dimethoxy-1*H*-1,3-benzodiazol-1-yl)-3-[[4-hydroxy-5-(methoxycarbonyl)thiophen-2-yl]oxy]thiophene-2-carboxylate (7a, $C_{21}H_{18}N_2O_8S_2$) was isolated as a byproduct of compound **6** synthesis as golden powder. Yield 1.35 g (4%); m.p.: 204–205 °C; ^{1}H NMR (400 MHz, DMSO-d_6): δ = 10.75 (br.s, 1H), 9.98 (br.s, 1H), 8.00 (s, 1H), 7.27 (s, 1H,), 6.69 (s, 1H), 6.59 (s, 1H), 3.91 (s, 3H), 3.85 (s, 3H), 3.72 (s, 6H) ppm; ^{13}C NMR (75 MHz, DMSO-d_6): δ = 162.63, 162.18, 159.62, 156.82, 147.85, 146.90, 141.88, 136.25, 135.57, 134.48, 127.50, 122.25, 119.87, 105.22,

Scheme 1

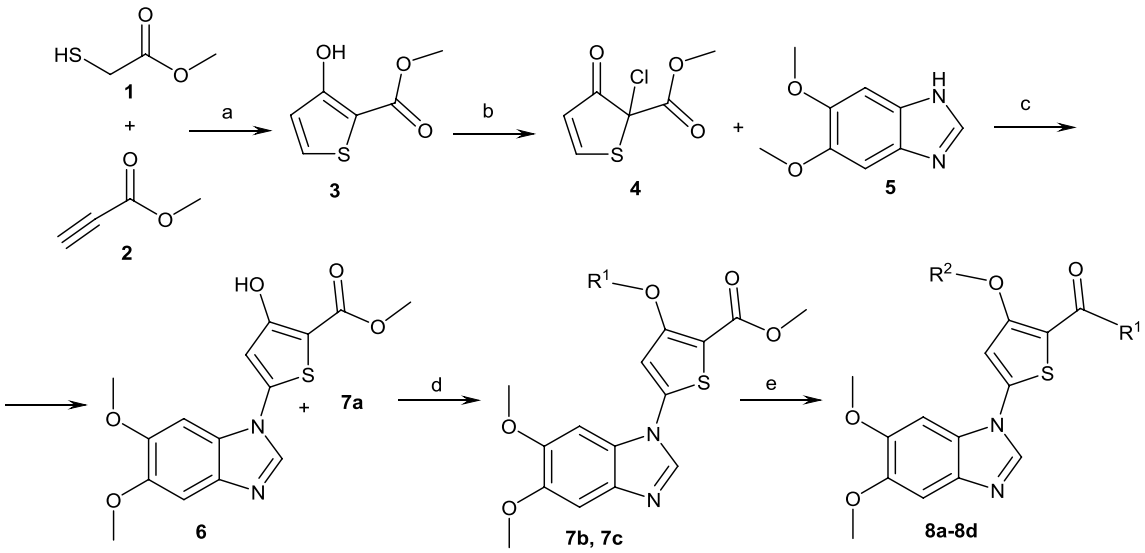

103.49, 102.28, 93.33, 55.88, 55.85, 52.18, 51.41 ppm; LC–MS (ESI): $t_r = 0.961$, $m/z = 491.0$ ($[M+H]^+$).

Methyl 5-(5,6-dimethoxy-1*H*-1,3-benzodiazol-1-yl)-3-[[2-(methanesulfonyl)phenyl]methoxy]thiophene-2-carboxylate (7b, $C_{23}H_{22}N_2O_7S_2$) To the 3.35 g of **6** (0.01 mol) and 2 g of K_2CO_3, 30 cm^3 of DMF were added under stirring following with 2.1 g of 2-(methylsulfonyl)benzyl chloride (0.01 mol). Stirring continued overnight and 150 cm^3 of water were added. **7b** that precipitated was collected by filtration, washed with water, and dried. Yield 4.5 g (89%); white powder; m.p.: 184–185 °C; ^{1}H NMR (400 MHz, DMSO-d_6): $\delta = 8.39$ (s, 1H), 8.04 (d, 1H, $J = 7.3$ Hz), 7.92 (d, 1H, $J = 7.6$ Hz), 7.79 (t, 1H, $J = 7.5$ Hz), 7.67 (t, 1H, $J = 7.3$ Hz), 7.64 (s, 1H), 7.25 (s, 2H), 5.75 (s, 2H), 3.89 (s, 3H), 3.86 (s, 3H), 3.79 (s, 3H), 3.10 (s, 3H) ppm; ^{13}C NMR (75 MHz, DMSO-d_6): $\delta = 160.69$, 158.91, 148.86, 147.11, 141.19, 141.05, 138.51, 136.94, 134.59, 134.13, 130.71, 129.59, 129.56, 125.89, 110.36, 103.12, 102.57, 94.12, 70.37, 56.0, 55.91, 51.72, 44.36 ppm; LC–MS (ESI): $t_r = 0.917$, $m/z = 503.0$ ($[M+H]^+$).

Methyl 5-(5,6-dimethoxy-1*H*-1,3-benzodiazol-1-yl)-3-[[4-(methanesulfonyl)phenyl]methoxy]thiophene-2-carboxylate (7c, $C_{23}H_{22}N_2O_7S_2$) was obtained by similar procedure with **7b** but using 2.7 g of 4-(methylsulfonyl)benzyl bromide (0.11 mol) instead of 2-(methylsulfonyl)benzyl chloride. Yield 4.8 g (96%); yellow powder; m.p.: 196–197 °C; ^{1}H NMR (400 MHz, DMSO-d_6): $\delta = 8.46$ (s, 1H), 7.99 (d, 2H, $J = 7.8$ Hz), 7.78 (d, 2H, $J = 7.8$ Hz), 7.64 (s, 1H), 7.34 (s, 1H), 7.22 (s, 1H), 5.54 (s, 2H), 3.84 (s, 3H), 3.83 (s, 3H), 3.82 (s, 3H), 3.23 (s 3H) ppm; ^{13}C NMR (75 MHz, DMSO-d_6): $\delta = 160.72$, 158.93, 147.83, 147.11, 142.25, 141.15, 140.87, 140.20, 136.91, 127.50, 127.17, 125.86, 110.56, 103.84, 102.56, 94.13, 71.8, 56.10, 55.91, 51.77, 43.48 ppm; LC–MS (ESI): $t_r = 0.846$, $m/z = 503.0$ ($[M+H]^+$).

5-(5,6-Dimethoxy-1*H*-1,3-benzodiazol-1-yl)-3-[[2-(methanesulfonyl)phenyl]methoxy]thiophene-2-carboxylic acid (8a, $C_{22}H_{20}N_2O_7S_2$) 4.03 g of **7b** (0.008 mol) and 1 g of KOH were dissolved in 15 cm^3 of dimethyl sulfoxide and mixture allowed to stand at with respect to overnight. 100 cm^3 of water were added, solution was treated with charcoal, and **8a** precipitated by the addition of hydrochloric acid. **8a** was filtered off and dried to give 3.05 g (78%) of beige powder. M.p.: 233–234 °C; ^{1}H NMR (400 MHz, DMSO-d_6): $\delta = 12.8$ (br.s 1H), 9.40 (s, 1H), 8.02 (d, 1H, $J = 7.8$ Hz), 7.92 (d, 1H, $J = 7.6$ Hz), 7.78 (br.s, 2H), 7.64 (s, 1H), 7.35 (s, 1H), 7.29 (s, 1H), 5.73 (s, 2H), 3.90 (s, 6H), 3.29 (s, 3H) ppm; ^{13}C NMR (75 MHz, DMSO-d_6): $\delta = 161.89$, 158.12, 147.82, 147.07, 141.23, 140.23, 138.62, 136.88, 134.75, 134.10, 130.89, 129.64, 129.56, 126.00, 110.73, 105.29, 102.55, 94.04, 70.31, 56.02, 55.93, 44.41 ppm; LC–MS (ESI): $t_r = 0.795$, $m/z = 488.8$ ($[M+H]^+$).

5-(5,6-Dimethoxy-1*H*-1,3-benzodiazol-1-yl)-3-[[2-(methanesulfonyl)phenyl]methoxy]thiophene-2-carboxamide (8b, $C_{22}H_{21}N_3O_6S_2$) To the suspension of 1 g of **8a** (0.002 mol) in 200 cm^3 of dry CH_2Cl_2, 0.3 cm^3 of thionyl chloride (0.004 mol) were added and mixture refluxed for 2 h under stirring. During this time mixture turned to clear solution, later, new precipitate formed. Methylene chloride removed under reduced pressure and 25 cm^3 of solution of ammonia in dry DMF were added. Dilution with water precipitated obtained amide **8b** as a beige powder. Yield 0.76 g (76%); m.p.: 236–237 °C; ^{1}H NMR (400 MHz, DMSO-d_6): $\delta = 8.37$

(s, 1H), 8.03 (d, 1H, $J=7.6$ Hz), 7.84 (d, 2H, $J=7.3$ Hz), 7.81 (t, 2H, $J=7.2$ Hz), 7.68 (t, 1H, $J=7.3$ Hz), 7.56 (br.s, 1H), 7.30 (s, 1H), 7.19 (s, 1H), 7.08 (br.s, 1H), 5.82 (s, 2H), 3.87 (s, 6H), 3.28 (s, 3H) ppm; ^{13}C NMR (75 MHz, DMSO-d_6): $\delta=164.73$, 158.37, 147.28, 147.03, 141.13, 140.86, 138.59, 136.71, 134.69, 134.11, 130.33, 129.60, 129.57, 125.94, 110.58, 105.28, 102.51, 94.08, 70.46, 56.04, 55.95, 44.40 ppm; LC–MS (ESI): $t_r=0.768$, $m/z=488.0$ ($[M+H]^+$).

5-(5,6-Dimethoxy-1*H*-1,3-benzodiazol-1-yl)-3-[[4-(methanesulfonyl)phenyl]methoxy]-*N*,*N*-dimethylthiophene-2-carboxamide (8c, $C_{24}H_{25}N_3O_6S_2$) Synthesis was carried out following procedure similar to described for the synthesis of **8b** starting from 1 g of **7c** using solution of dimethylamine in dry DMF. Yield 67%; light brown powder; m.p.: 176–177 °C; ^{1}H NMR (400 MHz, DMSO-d_6): $\delta=7.97$ (d, 2H, $J=7.3$ Hz), 7.90 (s, 1H), 7.61 (d, 2H, $J=7.3$ Hz), 7.29 (s, 1H), 7.26 (s, 1H), 7.05 (s, 1H), 6.83 (s, 1H), 5.26 (s, 2H), 3.95 (s, 3H), 3.92 (s, 3H), 3.14 (s, 6H), 3.07 (s, 3H) ppm; ^{13}C NMR (75 MHz, DMSO-d_6): $\delta=161.76$, 151.29, 147.74, 146.98, 142.15, 141.40, 140.35, 137.24, 136.74, 128.07, 127.23, 126.35, 111.19, 110.63, 102.46, 93.80, 71.97, 56.03, 55.91, 43.44, 39.11, 37.72 ppm; LC–MS (ESI): $t_r=0.787$, $m/z=516.0$ ($[M+H]^+$).

5-(5,6-Dimethoxy-1*H*-1,3-benzodiazol-1-yl)-3-[[4-(methanesulfonyl)phenyl]methoxy]thiophene-2-carboxylic acid (8d, $C_{22}H_{20}N_2O_7S_2$) Synthesis was carried out following procedure, described for the synthesis of **8a**. Yield 2.97 g (76%); brown powder; m.p.: 231–232 °C; ^{1}H NMR (400 MHz, DMSO-d_6): $\delta=12.80$ (br.s, 1H), 8.44 (s, 1H), 7.97 (d, 2H, $J=7.9$ Hz), 7.78 (d, 2H, $J=8.0$ Hz), 7.59 (s, 1H), 7.34 (s, 1H), 7.22 (s, 1H), 5.50 (s, 2H), 3.84 (s, 6H), 3.22 (s, 3H) ppm; ^{13}C NMR (75 MHz, DMSO-d_6): $\delta=161.93$, 152.35, 147.87, 147.06, 142.21, 141.34, 140.64, 138.53, 136.97, 127.91, 127.19, 126.04, 110.81, 107.33, 102.51, 93.95, 71.16, 56.07, 55.96, 43.50 ppm; LC–MS (ESI): $t_r=0.783$, $m/z=488.8$ ($[M+H]^+$).

Molecular docking

Molecular docking of compounds into the ATP-binding site of FGFR1 (crystal structure with PDB accession code 3GQI) was performed using AutoDock 4.2 software [53]. Water molecules and ligand were removed from the PDB file of receptor. The hydrogen atoms and Gasteiger partial charges were added by AutoDockTools-1.5.6 software [54].

The ligands were converted in 3D coordinates with minimization and Gasteiger partial charges were added using the software package Vega ZZ [55]. Docking was carried out with default parameters into FGFR1 ATP-binding pocket [53]. The coordinates of gridcenter were: −33.568; 29.207; 36.27, the dimensions of search grid: 36; 42; 52, the spacing was 0.375 Å. The top scored complexes from virtual screening were visually inspected using Discovery Studio Visualizer 4.0 [56].

Kinase assay

The FGFR1 kinase assays were performed in reaction mixture with total volume of 30 mm^3 containing 10 mM MOPS (pH 7.2), 0.1 mM sodium orthovanadate, 0.2 mM EDTA, 0.002% Brij 35, 0.2 mg/cm^3 BSA, 0.02% β-mercaptoethanol, 250 µM of peptide substrate (KKKSPGEYVNIEFG, GenScript), various concentrations of inhibitor dissolved in DMSO (final DMSO concentration in probe less than 1%), and 10 mU of recombinant FGFR1 enzyme (Millipore, Cat. N. 14–582). The reaction was initiated by the addition of ATP (50 µM ATP, 25 mM MgAc containing 0.1 µCi of [γ-32P]ATP per probe) and samples incubated at 30 °C for 25 min. The reaction was terminated by the addition of 5% phosphoric acid and the precipitation of material onto phosphocellulose filters "Whatman P81". Filters were washed three times with 0.75% phosphoric acid and the incorporation of [^{32}P] into the peptide substrate was determined by counting the radioactivity retained on the filters in a PerkinElmer scintillation counter. Kinase residual activity was expressed in percentages to DMSO control. The concentration of compound that inhibited enzymatic activity by 50% (IC_{50}) was determined graphically. The titration curves were built in coordinates of lg[C] µM and CPM. lg[C] for the mean value of CPM in the point half between upper and lower asymptotes was determined. The inverse logarithm of inhibitor concentration in this point was taken as IC_{50} value.

Cellular proliferation assay

Jurkat cell (Russian Cell Culture Collection) viability was examined using a standard MTT assay [57]. Cells were grown in DMEM containing 10% fetal bovine serum (FBS), 100 mg/cm^3 penicillin, and 100 mg/cm^3 streptomycin in humidified air at 37 °C with 5% CO_2. Viable cells were seeded into 96-well tissue plate at 2×10^5 cells/cm^3 preincubated for 24 h and treated with the synthesized compounds (compounds in DMSO solution, final DMSO concentration less than 0.5%) at various concentrations. After 72 h treatment, the cells were incubated with 15 mm^3 MTT (3-(4,5-dimethyl-thiazol-2-yl)-2,5-diphenyl-tetrazolium bromide from Sigma) solution (5 mg/cm^3) for 4 h at 37 °C, 5% CO_2. The formazan precipitates were dissolved in 200 mm^3 DMSO, and the absorbance at 540 nm of each well was measured by spectrofluorometer MR 700 (Dynatech). The cell viability was expressed as a percentage relative to the untreated control cells.

Acknowledgements This work was supported by the Grant from the National Academy of Sciences of Ukraine (0117U000204).

References

1. Turner N, Grose R (2010) Nat Rev Cancer 10:116
2. Heist RS, Mino-Kenudson M, Sequist LV, Tammireddy S, Morrissey L, Christiani DC, Engelman JA, Iafrate AJ (2012) J Thorac Oncol 7:1775
3. Jiang T, Gao G, Fan G, Li M, Zhou C (2015) Lung Cancer 87:1
4. Young RJ, Lim AM, Angel C, Collins M, Deb S, Corry J, Wiesenfeld D, Kleid S, Sigston E, Lyons B, Russell PA, Wright G, McArthur GA, Fox SB, Rischin D, Solomon B (2013) Oral Oncol 49:576
5. Schröck A, Göke F, Wagner P, Bode M, Franzen A, Huss S, Agaimy A, Ihrler S, Kirsten R, Kristiansen G, Bootz F, Lengerke C, Perner S (2014) Head Neck 36:1253
6. Xu C, Li W, Qiu P, Xia Y, Du X, Wang F, Shen L, Chen Q, Zhao Y, Jin R, Wu J, Liang G, Li X (2015) Anticancer Drugs 26:379
7. Lehnen NC, von Mässenhausen A, Kalthoff H, Zhou H, Glowka T, Schütte U, Höller T, Riesner K, Boehm D, Merkelbach-Bruse S, Kirfel J, Perner S, Gütgemann I (2013) Histopathology 63:157
8. Kwak Y, Nam SK, Seo AN, Kim DW, Kang SB, Kim WH, Lee HS (2015) Pathobiology 82:76
9. Arber DA, Orazi A, Hasserjian R, Thiele J, Borowitz MJ, Le Beau MM, Bloomfield CD, Cazzola M, Vardiman JW (2016) Blood 127:2391
10. Patnaik M, Gangat N, Knudson RA, Keefe JG, Hanson CA, Pardanani A, Ketterling RP, Tefferi A (2010) Am J Hematol 85:238
11. Wei M, Peng X, Xing L, Dai Y, Huang R, Geng M, Zhang A, Ai J, Song Z (2018) Eur J Med Chem 154:9
12. Xie Z, Cheng D, Luo L, Shen G, Pan S, Pan Y, Chen B, Wang X, Liu Z, Zhang Y, Ye F (2018) J Enzyme Inhib Med Chem 33:905
13. Jiang A, Liu Q, Wang R, Wei P, Dai Y, Wang X, Xu Y, Ma Y, Ai J, Shen J, Ding J, Xiong B (2018) Molecules 23:E698
14. Zhang Y, Liu H, Zhang Z, Wang R, Liu T, Wang C, Ma Y, Ai J, Zhao D, Shen J, Xiong B (2017) Molecules 22:E583
15. Turner LD, Summers AJ, Johnson LO, Knowles MA, Fishwick CWG (2017) ACS Med Chem Lett 8:1264
16. Cui J, Peng X, Gao D, Dai Y, Ai J, Li Y (2017) Bioorg Med Chem Lett 27:3782
17. Zhang Z, Zhao D, Dai Y, Cheng M, Geng M, Shen J, Ma Y, Ai J, Xiong B (2016) Molecules 21:E1407
18. Liu J, Peng X, Dai Y, Zhang W, Ren S, Ai J, Geng M, Li Y (2015) Org Biomol Chem 13:7643
19. Yan W, Wang X, Dai Y, Zhao B, Yang X, Fan J, Gao Y, Meng F, Wang Y, Luo C, Ai J, Geng M, Duan W (2016) J Med Chem 59:6690
20. Ebiike H, Taka N, Matsushita M, Ohmori M, Takami K, Hyohdoh I, Kohchi M, Hayase T, Nishii H, Morikami K, Nakanishi Y, Akiyama N, Shindoh H, Ishii N, Isobe T, Matsuoka H (2016) J Med Chem 59:10586
21. Guo P, Xie Z, Zhang H, Zhang Z, Han C, Cheng D, Lin D, Zhang Y, Wang X, Guo X, Ye F (2017) Med Chem 13:753
22. Wang X, Chen D, Yu S, Zhang Z, Wang Y, Qi X, Fu W, Xie Z, Ye F (2016) Chem Biol Drug Des 87:499
23. Gryshchenko AA, Bdzhola VG, Balanda AO, Briukhovetska NV, Kotey IM, Golub AG, Ruban TP, Lukash LL, Yarmoluk SM (2015) Bioorg Med Chem 23:2287
24. Ekkati AR, Madiyan V, Ravindranathan KP, Bae JH, Schlessinger J, Jorgensen WL (2011) Tetrahedron Lett 52:2228
25. Zhu W, Chen H, Wang Y, Wang J, Peng X, Chen X, Gao Y, Li C, He Y, Ai J, Geng M, Zheng M, Liu H (2017) J Med Chem 60:6018
26. Zhao B, Li Y, Xu P, Dai Y, Luo C, Sun Y, Ai J, Geng M, Duan W (2016) ACS Med Chem Lett 7:629
27. Li X, Guise CP, Taghipouran R, Yosaatmadja Y, Ashoorzadeh A, Paik WK, Squire CJ, Jiang S, Luo J, Xu Y, Tu ZC, Lu X, Ren X, Patterson AV, Smaill JB, Ding K (2017) Eur J Med Chem 135:531
28. Oguro Y, Miyamoto N, Takagi T, Okada K, Awazu Y, Miki H, Hori A, Kamiyama K, Imamura S (2010) Bioorg Med Chem 18:7150
29. Ye F, Wang Y, Nian S, Wang Y, Chen D, Yu S, Wang S (2015) J Enzyme Inhib Med Chem 30:961
30. Panek RL, Lu GH, Dahring TK, Batley BL, Connolly C, Hamby JM, Brown KJ (1998) J Pharmacol Exp Ther 286:569
31. Łazarenkow A, Michalska M, Mirowski M, Słomiak K, Nawrot-Modranka J (2017) Acta Biochim Pol 64:585
32. Liu Z, Yu S, Chen D, Shen G, Wang Y, Hou L, Lin D, Zhang J, Ye F (2016) Drug Des Dev Ther 10:1489
33. Fan J, Dai Y, Shao J, Peng X, Wang C, Cao S, Zhao B, Ai J, Geng M, Duan W (2016) Bioorg Med Chem Lett 26:2594
34. Chen CH, Liu YM, Pan SL, Liu YR, Liou JP, Yen Y (2016) Oncotarget 7:26374
35. Ye F, Chen L, Hu L, Xiao T, Yu S, Chen D, Wang Y, Liang G, Liu Z, Wang S (2015) Bioorg Med Chem Lett 25:1556
36. Chen G, Weng Q, Fu L, Wang Z, Yu P, Liu Z, Li X, Zhang H, Liang G (2014) Bioorg Med Chem 22:6953
37. Zsákai L, Németh G, Szántai-Kis C, Greff Z, Horváth Z, Szokol B, Baska F, Boon TC, Orfi L, Kéri G (2013) Acta Pharm Hung 83:47
38. Kumar BV, Lakshmi N, Kumar MR, Rambabu G, Manjashetty TH, Arunasree KM, Sriram D, Ramkumar K, Neamati N, Dayam R, Sarma JA (2014) Curr Top Med Chem 14:2031
39. Wu J, Ji J, Weng B, Qiu P, Kanchana K, Wei T, Wang Y, Cai Y, Li X, Liang G (2014) Oncotarget 5:4543
40. Gryshchenko AA, Levchenko KV, Bdzhola VG, Ruban TP, Lukash LL, Yarmoluk SM (2015) J Enzyme Inhib Med Chem 30:126
41. Chen Z, Wang X, Zhu W, Cao X, Tong L, Li H, Xie H, Xu Y, Tan S, Kuang D, Ding J, Qian X (2011) J Med Chem 54:3732
42. Thompson AM, Delaney AM, Hamby JM, Schroeder MC, Spoon TA, Crean SM, Showalter HD, Denny WA (2005) J Med Chem 48:4628
43. Borzilleri RM, Zheng X, Qian L, Ellis C, Cai ZW, Wautlet BS, Mortillo S, Jeyaseelan RSr, Kukral DW, Fura A, Kamath A, Vyas V, Tokarski JS, Barrish JC, Hunt JT, Lombardo LJ, Fargnoli J, Bhide RS (2005) J Med Chem 48:3991
44. Gryshchenko AA, Tarnavskiy SS, Levchenko KV, Bdzhola VG, Volynets GP, Golub AG, Ruban TP, Vygranenko KV, Lukash LL, Yarmoluk SM (2016) Bioorg Med Chem 24:2053
45. Pal SK, Rosenberg JE, Hoffman-Censits JH, Berger R, Quinn DI, Galsky MD, Wolf J, Dittrich C, Keam B, Delord JP, Schellens JHM, Gravis G, Medioni J, Maroto P, Sriuranpong V, Charoentum C, Burris HA, Grünwald V, Petrylak D, Vaishampayan U, Gez E, De Giorgi U, Lee JL, Voortman J, Gupta S, Sharma S, Mortazavi A, Vaughn DJ, Isaacs R, Parker K, Chen X, Yu K, Porter D, Graus Porta D, Bajorin DF (2018) Cancer Discov 8:812
46. Tabernero J, Bahleda R, Dienstmann R, Infante JR, Mita A, Italiano A, Calvo E, Moreno V, Adamo B, Gazzah A, Zhong B, Platero SJ, Smit JW, Stuyckens K, Chatterjee-Kishore M, Rodon J, Peddareddigari V, Luo FR, Soria JC (2015) J Clin Oncol 33:3401
47. Yoza K, Himeno R, Amano S, Kobashigawa Y, Amemiya S, Fukuda N, Kumeta H, Morioka H, Inagaki F (2016) Genes Cells 21:1049
48. Bamborough P, Christopher JA, Cutler GJ, Dickson MC, Mellor GW, Morey JV, Patel CB, Shewchuk LM (2006) Bioorg Med Chem Lett 16:6236
49. Emmitte KA, Andrews CW, Badiang JG, Davis-Ward RG, Dickson HD, Drewry DH, Emerson HK, Epperly AH, Hassler DF,

Knick VB, Kuntz KW, Lansing TJ, Linn JA Jr, Mook RA, Nailor KE, Salovich JM, Spehar GM, Cheung M (2009) Bioorg Med Chem Lett 19:1018
50. Armstrong E, Vainikka S, Partanen J, Korhonen J, Alitalo R (1992) Cancer Res 52:2004
51. Fiesselmann H, Pfeiffer G (1954) Chem Ber 87:848
52. Corral C, Lissavetzky J (1984) Synthesis 10:847
53. AutoDock 4.2 User Guide. http://autodock.scripps.edu/faqs-help/manual/autodock-4-2-user-guide/AutoDock4.2_UserGuide.pdf. Accessed 14 May 2019
54. Pedretti A, Villa L, Vistoli G (2004) J Comput Aided Mol Des 18:167
55. Morris GM, Huey R, Lindstrom W, Sanner MF, Belew RK, Goodsell DS, Olson AJ (2009) J Comput Chem 30:2785
56. Discovery Studio Visualizer 4.0. http://www.3dsbiovia.com/products/collaborative-science/biovia-discovery-studio/visualization-download.php. Accessed 14 May 2019
57. Mosmann T (1983) Methods 65:55